

## Research Article

# Restraining the Demand Side Power Fluctuation of Active Distribution Network Using $0^\circ/180^\circ$ Phase Controlled Electric Spring

Yixi Chen , Gang Ma , Guchao Xu, Huaiyi Chen, and Hang Zhang

*School of Electrical & Automation Engineering, Nanjing Normal University, Nanjing 210042, China*

Correspondence should be addressed to Gang Ma; [nnumg@njnu.edu.cn](mailto:nnumg@njnu.edu.cn)

Received 3 February 2018; Revised 13 May 2018; Accepted 28 May 2018; Published 2 July 2018

Academic Editor: Daniela Proto

Copyright © 2018 Yixi Chen et al. This is an open access article distributed under the Creative Commons Attribution License, which permits unrestricted use, distribution, and reproduction in any medium, provided the original work is properly cited.

In active distribution network, the random power output by wind/solar distributed generation may cause the stochastic fluctuation of demand side power, which will bring difficulties to power dispatching. In this paper, a method of restraining the demand side power fluctuation of active distribution network is proposed, in which a new power electronic device—electric spring—is applied by  $0^\circ/180^\circ$  phase control strategy. Firstly, the basic principles of electric spring are introduced. Secondly, the reason for demand side power fluctuation of active distribution network is analyzed. After that, the  $0^\circ/180^\circ$  phase control strategy of electric spring is proposed to restrain the demand side power fluctuation of active distribution network and the selection basis of noncritical loads is also obtained. The simulation results show that the method proposed in this paper is effective and the obtained selection basis of noncritical loads is reasonable.

## 1. Introduction

Energy saving and emission reduction have jointly promoted the development of renewable energy generation [1, 2]. As one of the main forms of renewable energy generation, distributed generation (DG) outputs fluctuant power due to the intermittent characteristic of renewable energy [3, 4].

Active distribution network (ADN) represents the distribution network containing DG, the demand side power of which mainly includes the output power of DG, and the input power of loads. The fluctuant power output by DG may cause the fluctuation of demand side power, and therefore the power dispatching will be difficult [5].

In order to control the demand side power effectively, some demand side management methods such as direct load control, real-time pricing, charging, and discharging by energy storage devices have been applied in distribution networks [6]. However, these methods have some weaknesses. The method direct load control switches on/off loads directly according to the amount of power supply and power demand, which is intrusive to consumers [7, 8]. The method real-time pricing can shape the load curve as desired at the macrolevel,

but it could not dispose of the demand side power fluctuation caused by DG [9, 10]. The method using energy storage devices can eliminate peak and fill valley for demand side power, but this approach needs to add much storage capacity when the fluctuation of DG is big, which is uneconomical [11, 12].

As a novel power electronic device, electric spring (ES) was at first used to restrain the bus voltage fluctuation caused by the access of DG, and the frequency adjustment function can be obtained simultaneously. Chen X. et al. [13] analyzed the function of ES to mitigate voltage and frequency fluctuation in microgrids. Lee CK. et al. [14] drew a conclusion that using ES to regulate mains voltage can reduce the energy storage requirements in future smart grid. Wang Q. et al. [15] proposed a novel  $\delta$  control strategy to improve the steady-state performance of ES. Yan S. et al. [16] proposed a new topology of ES by using back-to-back converter in order to extend its operating range. Moreover, the criteria and conditions for minimizing the average and oscillating power of the 3-ph ES are introduced in [17]. ES is evaluated for improving the fault-ride through capability of the wind turbine generation system with fixed speed induction generator

in [18]. In general, although there have been some research results of ES, however the potential of ES has not been fully tapped. As (1) current analysis of ES is chiefly focused on the voltage stabilizing function, more functions of ES should be derived. (2) Current use of ES is restricted to ensure the reactive power compensation function firstly; however,  $0^\circ/180^\circ$  phase control which is without the consideration of reactive power has not been studied and analyzed deeply.

In this paper, a method of restraining the demand side power fluctuation of ADN using  $0^\circ/180^\circ$  phase controlled ES is proposed. Firstly, the basic principles of ES are introduced. Then, the reason for demand side power fluctuation of ADN is analyzed. After that, the  $0^\circ/180^\circ$  phase control strategy of ES is proposed to restrain the demand side power fluctuation of active distribution network and the selection basis of noncritical loads is also obtained. At last, simulations are conducted to verify the effectiveness of the method proposed in this paper.

## 2. Analysis of ES Principles

Inspired by Hooke's law of mechanical spring, Hui SYR. et al. [19] proposed the concept of ES. Similar to the supporting function of mechanical spring, ES can stabilize the controlled variable effectively by controlling the power flow [20, 21].

As shown in Figure 1(a), ES consists of measurement module, control loop, PWM power inverter, and low-pass filter (i.e., filter inductance  $L_f$  and filter capacitance  $C_f$ ) [22, 23]. The measurement module measures voltage, current, and other real-time data of the distribution network and then sends them to the control loop. The control loop decides the required ES voltage based on the real-time data measured by the measurement module and sends it to the inverter as a modulation signal. Then the inverter generates the corresponding ES voltage according to the modulation signal.

What needs to be explained here is that the first generation of ES (ES-1) does not involve battery storage. It uses reactive power to stabilize the bus voltage. Version two (ES-2) utilizes batteries as energy storage, which allows the ES to output/absorb both active and reactive power. ES-3 applies bidirectional AC/DC converter with battery storage and without association with noncritical load [24]. For ES-1, as it does not have the ability of active power control, it is not applicable for this paper. For ES-3, as noncritical load is not applied, it can only increase the capacity of ES by simply increasing the capacity of batteries. For ES-2, as noncritical load is applied, it can increase the capacity of ES not only by increasing the capacity of batteries, but also by increasing the number of noncritical loads, which is obviously more suitable for this paper. Therefore, all of the 'ESs' mentioned in this paper are ES-2.

Loads can be divided into noncritical loads and critical loads according to different voltage stability requirements. For example, electric heaters, lighting systems, and small motors with no stalling problems (e.g., fans, ovens, dish washes, and dryers) can tolerate a relatively large voltage variation with little or no noticeable impact on the consumers. These loads can be set as noncritical loads [25]. Loads which require well-regulated mains voltage such as life-supporting

medical equipment and precision instrument can be set as critical loads [26]. As shown in Figure 1(b), ES is in series with a noncritical load to form a smart load, where  $V_{ES}$  is ES voltage,  $V_{NC}$  is noncritical load voltage,  $V_S$  is bus voltage (i.e., critical load voltage), and  $I_{SL}$  is smart load current.

As shown in Figure 1(b), the relationship of  $V_{ES}$ ,  $V_{NC}$ , and  $V_S$  can be obtained as

$$V_{ES} + V_{NC} = V_S \quad (1)$$

With the fluctuation of power output by DG, ES will change its voltage  $V_{ES}$  dynamically in order to maintain the stability of the controlled variable; therefore  $V_{NC}$  will change dynamically according to (1). That is to say, ES stabilizes the controlled variable by transferring its fluctuation to  $V_{NC}$ .

Now, ES has been deeply researched on in order to restrain the bus voltage fluctuation caused by the access of DG [27, 28]. In this application, (1) can be expressed by vector diagrams as shown in Figure 2, taking the noncritical load whose impedance angle is  $\varphi$  as an example. The phase angle difference between  $V_{ES}$  and  $I_{SL}$  is generally controlled to be  $\pm 90^\circ$ , in order that ES inputs/outputs reactive power only. When  $V_{ES}$  leads  $I_{SL}$   $90^\circ$ , ES works in inductive mode, as shown in Figure 2(a); in this mode, ES can input reactive power to depress the overhigh bus voltage. When  $V_{ES}$  lags  $I_{SL}$   $90^\circ$ , ES works in capacitive mode, as shown in Figure 2(b); in this mode, ES can output reactive power to raise the overflow bus voltage.

Current use of ES is restricted to ensure the reactive power compensation function firstly. When ES is used to control active and reactive power simultaneously, the power compensated by ES can be illustrated by Figure 3 [29].  $S_{max}$  is the maximum apparent power ES can compensate, which is restricted by the maximum value of  $V_{ES}$  amplitude. According to Figure 3, on the condition that the apparent power compensate value is constant, when the reactive power compensation amount of ES is large, it can compensate less active power (as  $S_2$  in Figure 3); when the reactive power compensation amount of ES is small, it can compensate more active power (as  $S_1$  in Figure 3). At present, as STATCOM can effectively adjust reactive power in distribution network, ES is not used to regulate reactive power in this paper; therefore the active power compensation range of ES can be maximized.

## 3. Reason for the Demand Side Power Fluctuation in ADN

**3.1. Analysis.** In order to study the method of restraining the demand side power fluctuation of ADN, the reason for demand side power fluctuation of ADN must be analyzed first.

Compared with the traditional distribution network, the demand side power of ADN not only includes the input power of loads but also includes the output power of DG. Due to the intermittent characteristic of renewable energy, the output power of DG will be fluctuant; therefore the demand side power of ADN can be expressed as

$$P_{DEM} = P_{Load} - [P_{DG-REF} + \Delta P_{DG}(t)] \quad (2)$$

where  $P_{Load}$  represents the input power of loads,  $P_{DG-REF}$  represents the reference value of the output power of DG,

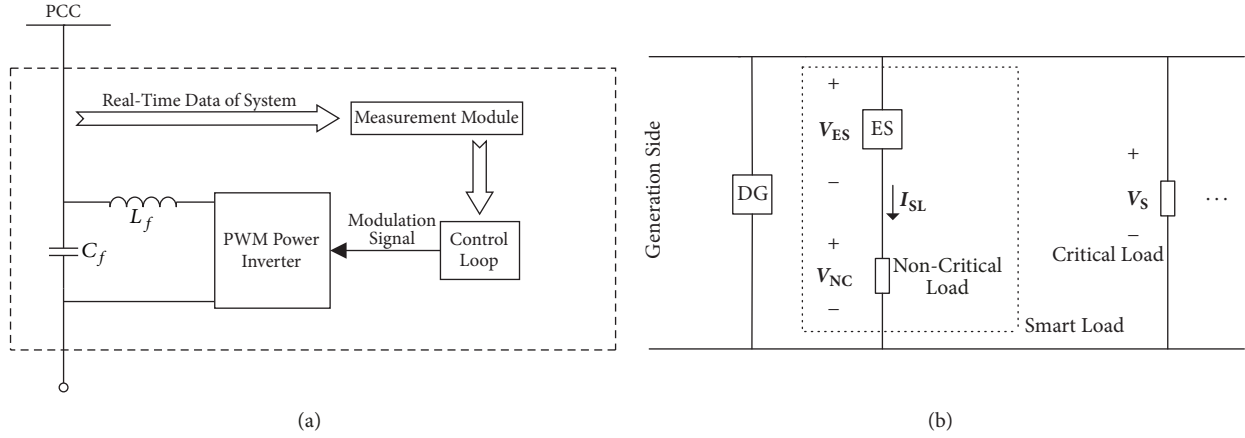


FIGURE 1: The basic structure and connection of ES. (a) Structure of ES. (b) Connection of ES.

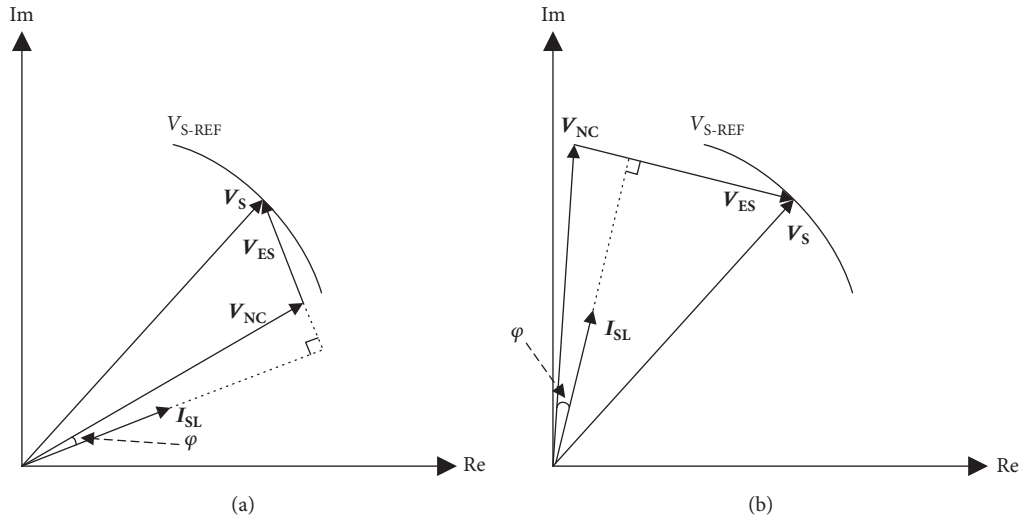


FIGURE 2: The vector diagram when ES is applied to restrain the bus voltage fluctuation caused by DG. (a) Inductive mode. (b) Capacitive mode.

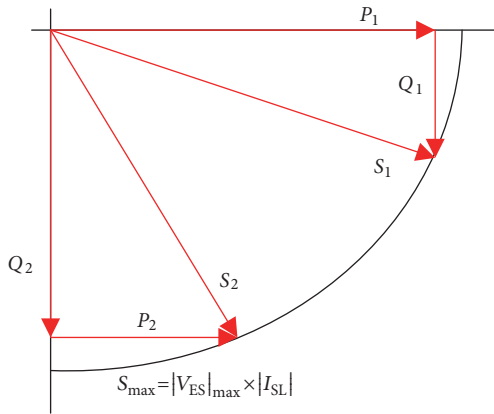


FIGURE 3: Illustration of power compensation by the ES.

and  $\Delta P_{DG}(t)$  represents the fluctuation quantity of DG output power comparing with  $P_{DG-REF}$ . In order to simplify the

analysis, the line loss which accounts for a relatively small proportion in the demand side power is not considered in this paper.

The selection range of  $P_{DG-REF}$  in (2) is

$$P_{DG-REF} \in [0, P_{DG-MAX}] \quad (3)$$

where  $P_{DG-MAX}$  represents the maximum power DG can output.

Let

$$P_{DEM-REF} = P_{Load} - P_{DG-REF} \quad (4)$$

where  $P_{DEM-REF}$  represents the reference value of the demand side power of ADN.

Therefore, substituting (4) into (2) gives

$$P_{DEM} = P_{DEM-REF} - \Delta P_{DG}(t) \quad (5)$$

As shown in (5), due to the fluctuation quantity  $\Delta P_{DG}(t)$  of DG output power, the demand side power of ADN  $P_{DEM}$  will fluctuate randomly around  $P_{DEM-REF}$ , which will bring difficulties to power dispatching.

3.2. *Idea for Solution.* According to (2), the fluctuation of DG output power is  $\Delta P_{DG}(t)$ . In order to eliminate the influence of this fluctuation on demand side power, the same fluctuation  $\Delta P_{DG}(t)$  can be exerted to loads power  $P_{Load}$ , which can balance out the fluctuation quantity  $\Delta P_{DG}(t)$  caused by DG. According to this, (2) can be modified as

$$P_{DEM} = [P_{Load} + \Delta P_{DG}(t)] - [P_{DG-REF} + \Delta P_{DG}(t)] \quad (6)$$

Substituting (4) into (6) gives

$$P_{DEM} = P_{DEM-REF} \quad (7)$$

Comparing (7) with (5), it can be found that the fluctuation of demand side power caused by DG can be eliminated if the above idea is achieved and the demand side power of ADN can be stabilized at the reference value  $P_{DEM-REF}$ . Moreover, according to this idea, the power consumption will increase when the quantity of DG output power is large, while the power consumption will decrease when the quantity of DG output power is small; therefore the new control paradigm where demand follows generation can be realized.

#### 4. 0°/180° Phase Control Strategy of ES

In order to achieve the above idea, ES can be applied. As shown in Figure 1(b), ES is in series with a noncritical load to form a smart load. With the dynamic voltage  $V_{ES}$  generated by ES, the input power of smart load can be changed dynamically; therefore the loads power  $P_{Load}$  can be altered according to the idea above.

Different from the application of restraining bus voltage fluctuation, when restraining the fluctuation of demand side power caused by DG in ADN, ES can be set to control active power only. Therefore, the phase angle difference between  $V_{ES}$  and  $I_{SL}$  can be controlled to be 0°/180°. When the phase angle difference is 0°, ES works in resistive mode, while when the phase angle difference is 180°, ES works in negative resistive mode.

4.1. *ES in Series with Resistive Noncritical Load.* If ES is used to restrain the fluctuation of demand side power in ADN when it is in series with a resistive noncritical load, (1) can be expressed by vector diagrams as shown in Figure 4, where the dashed vectors  $V_{NC}$  and  $I_{SL}$  represent the noncritical load voltage and smart load current respectively on the condition that ES is not applied and the vectors  $V_{NC}'$  and  $I_{SL}'$  represent the noncritical load voltage and smart load current, respectively, on the condition that ES is applied.

As shown in Figure 4(a), when ES works in resistive mode,  $V_{NC}'$  is less than  $V_{NC}$ ; accordingly  $I_{SL}'$  is less than  $I_{SL}$  and the input power of smart load is decreased. As shown in Figure 4(b), when ES works in negative resistive mode,  $V_{NC}'$  is greater than  $V_{NC}$ ; accordingly  $I_{SL}'$  is greater than  $I_{SL}$  and the input power of smart load is increased.

According to Figure 4, if ES is not applied, the input power of smart load can be expressed as

$$P = V_{NC} \cdot I_{SL} = |V_{NC}| \times \left| \frac{V_{NC}}{R_{NC}} \right| \quad (8)$$

If ES is applied, the input power of smart load can be expressed as

$$P' = V_{NC}' \cdot I_{SL}' + V_{ES} \cdot I_{SL}' = |V_{NC}| \times \left| \frac{(V_S - V_{ES})}{R_{NC}} \right| \quad (9)$$

Therefore, the adjustment of smart load input power produced by ES can be obtained as

$$\begin{aligned} \Delta P &= P - P' = |V_{NC}| \times \left( \left| \frac{V_{NC}}{R_{NC}} \right| - \left| \frac{(V_S - V_{ES})}{R_{NC}} \right| \right) \\ &= |V_{NC}| \times \left( \frac{(|V_{NC}| - |V_S - V_{ES}|)}{|R_{NC}|} \right) \end{aligned} \quad (10)$$

where  $|V_{NC}|$  is the noncritical load voltage if ES is not activated, which is equal to the bus voltage (the bus voltage is assumed to be constant in this paper).  $\Delta P > 0$  means that the phase angle difference between  $V_{ES}$  and  $I_{SL}$  is 0° and the input power of smart load is decreased by ES, while  $\Delta P < 0$  means that the phase angle difference between  $V_{ES}$  and  $I_{SL}$  is 180° and the input power of smart load is increased by ES.

4.2. *ES in Series with Resistive-Inductive Noncritical Load.* If ES is used to restrain the fluctuation of demand side power in ADN when it is in series with a resistive-inductive noncritical load, (1) can be expressed by vector diagrams as shown in Figure 5, where the impedance angle of noncritical load is  $\varphi$  and  $\theta$  is the difference angle between  $V_{NC}$  and  $V_S$ .

Similar to the above analysis, according to Figure 5, the input power of smart load, if ES is not applied, can be expressed as

$$P = V_{NC} \cdot I_{SL} = |V_{NC}| \times \left| \frac{V_{NC}}{Z_{NC}} \right| \times \cos \varphi \quad (11)$$

If ES is applied, the input power of smart load can be expressed as

$$\begin{aligned} P' &= V_{NC}' \cdot I_{SL}' + V_{ES} \cdot I_{SL}' \\ &= |V_{NC}'| \times \left| \frac{(V_S - V_{ES})}{Z_{NC}} \right| \times \cos \varphi + |V_{ES}| \\ &\quad \times \left| \frac{(V_S - V_{ES})}{Z_{NC}} \right| \\ &= |V_S| \times \left| \frac{(V_S - V_{ES})}{Z_{NC}} \right| \times \cos(\varphi - \theta) \end{aligned} \quad (12)$$

Therefore, the adjustment of smart load input power produced by ES can be obtained as

$$\begin{aligned} \Delta P &= P - P' \\ &= |V_{NC}| \times \left| \frac{V_{NC}}{Z_{NC}} \right| \times \cos \varphi - |V_S| \times \left| \frac{(V_S - V_{ES})}{Z_{NC}} \right| \\ &\quad \times \cos(\varphi - \theta) \end{aligned}$$

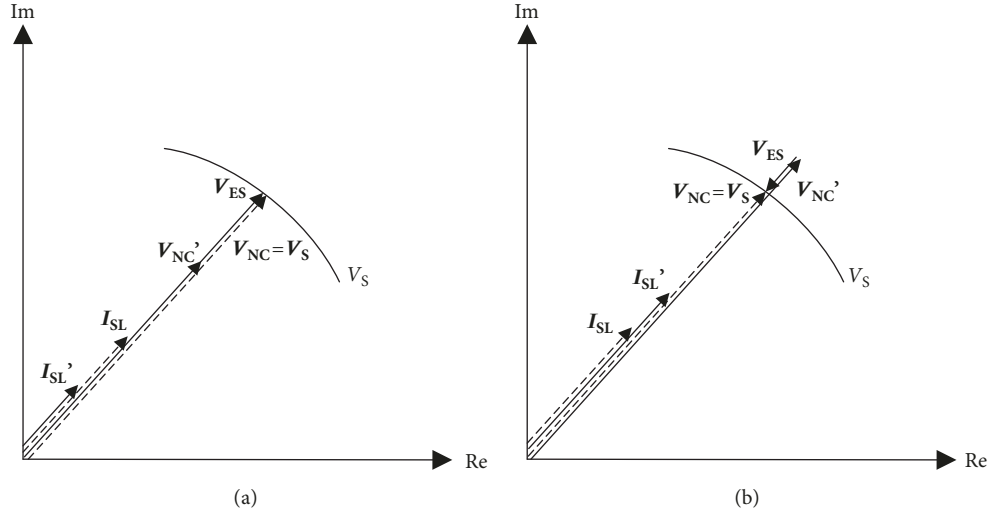


FIGURE 4: The vector diagram when ES is applied to restrain the demand side power fluctuation while noncritical load is resistive. (a) Resistive mode. (b) Negative resistive mode.

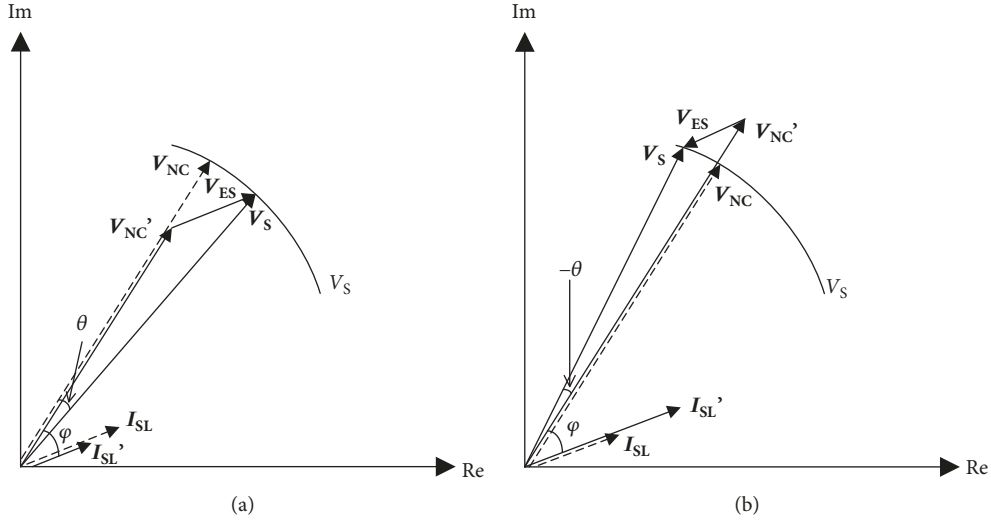


FIGURE 5: The vector diagram when ES is applied to restrain the demand side power fluctuation while noncritical load is resistive-inductive. (a) Resistive mode. (b) Negative resistive mode.

$$\begin{aligned}
 &= |\mathbf{V}_{NC}| \\
 &\times \left( \left| \frac{\mathbf{V}_{NC}}{Z_{NC}} \right| \times \cos \varphi - \left| \frac{(\mathbf{V}_S - \mathbf{V}_{ES})}{Z_{NC}} \right| \times \cos(\varphi - \theta) \right) \\
 &= |\mathbf{V}_{NC}| \\
 &\times \left( \frac{(|\mathbf{V}_{NC}| \cos \varphi - |\mathbf{V}_S - \mathbf{V}_{ES}| \cos(\varphi - \theta))}{|Z_{NC}|} \right) \tag{13}
 \end{aligned}$$

Same as (10),  $\Delta P > 0$  means that the input power of smart load is decreased by ES, while  $\Delta P < 0$  means that the input power of smart load is increased by ES.

4.3. *ES in Series with Resistive-Capacitive Noncritical Load.* If ES is used to restrain the fluctuation of demand side power in

ADN when it is in series with a resistive-capacitive noncritical load, (1) can be expressed by vector diagrams as shown in Figure 6, where the impedance angle of noncritical load is  $-\varphi$  and  $\theta$  is the difference angle between  $\mathbf{V}_S$  and  $\mathbf{V}_{NC}$ .

Same as the analysis of “ES in series with resistive-inductive noncritical load,” according to Figure 6, it can be obtained that the input power of smart load, if ES is not applied, can also be expressed as (11), the input power of smart load, if ES is applied, can also be expressed as (12), and the adjustment of smart load input power produced by ES can also be expressed as (13).

Based on the analysis above, (10) can be summarized as a special case of (13) ( $\varphi = \theta = 0^\circ$ ); that is, no matter what kinds of noncritical load is in series with ES to form a smart load, the adjustment of smart load input power produced by ES can all be expressed as (13). According to (13), ES can produce an

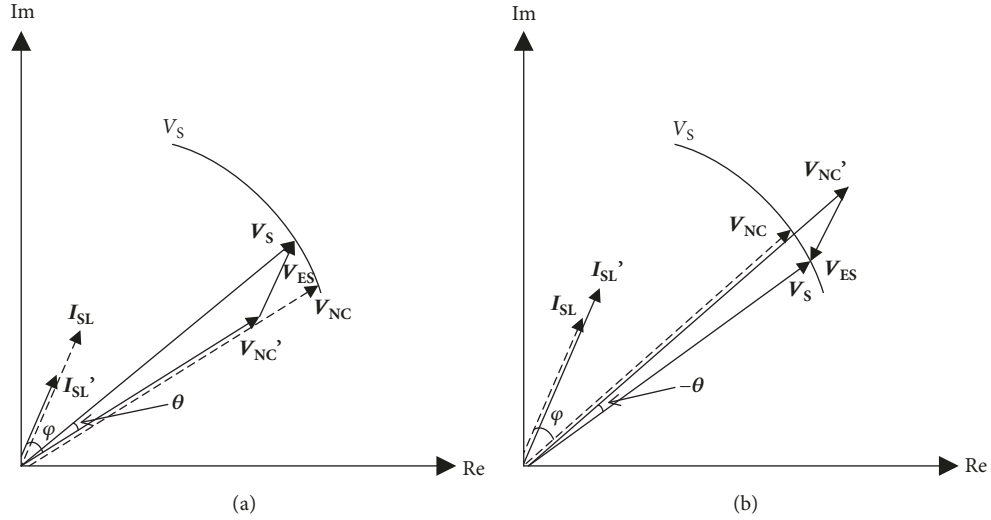


FIGURE 6: The vector diagram when ES is applied to restrain the demand side power fluctuation while noncritical load is resistive-capacitive. (a) Resistive mode. (b) Negative resistive mode.

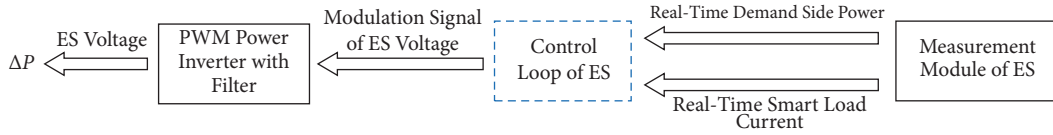


FIGURE 7: The flowchart of using ES to restrain the fluctuation of demand side power in ADN.

adjustment  $\Delta P$  for smart load input power by generating the voltage  $V_{ES}$ . Assume that the input power of loads, if ES is not applied, is  $P_{Load}$ ; therefore the input power of loads, if ES is applied, should be  $P_{Load} - \Delta P$  and (2) will change to be

$$P_{DEM} = [P_{Load} - \Delta P] - [P_{DG-REF} + \Delta P_{DG}(t)] \quad (14)$$

If  $\Delta P$  equals to  $-\Delta P_{DG}(t)$ , (14) can be equivalent to (6) and (7), the fluctuation of demand side power caused by DG can be eliminated, the demand side power of ADN  $P_{DEM}$  can be stabilized at the reference value  $P_{DEM-REF}$ , and the difficulties of power dispatching caused by the output power fluctuation of DG can be relieved.

**4.4. Selection Basis of Noncritical Loads.** According to the  $0^\circ/180^\circ$  phase control strategy above, when ES is used to restrain the fluctuation of demand side power caused by DG, no matter what kinds of noncritical load is in series with ES, the adjustment of smart load input power produced by ES can all be expressed as (13), which can be transformed to be

$$|V_S - V_{ES}| = \frac{[|V_{NC}| \times \cos \varphi - (\Delta P / |V_{NC}|) \times |Z_{NC}|]}{\cos(\varphi - \theta)} \quad (15)$$

According to (15), to achieve same  $\Delta P$ , bigger impedance modulus of noncritical load means that ES needs to generate bigger voltage, on the condition that the impedance angle of noncritical load is constant. However, according to the basic principles of PWM inverter, the value range of ES voltage is

constrained by the magnitude of DC voltage. Therefore, as the DC voltage is constant, in order to achieve stronger ability to restrain the fluctuation of demand side power caused by DG, noncritical loads which have smaller impedance modulus should be considered to be in series with ES firstly.

## 5. Control Loop Design

Based on the analysis above, the flowchart of using ES to restrain the fluctuation of demand side power in ADN can be expressed as Figure 7. As shown in Figure 7, the control loop of ES is the core part of the whole framework. In order to obtain a reasonable ES voltage modulation signal based on the real-time data, specific control loop needs to be designed.

**5.1. Control Loop of the Amplitude of ES Voltage.** According to the "idea for solution" and the  $0^\circ/180^\circ$  phase control strategy analyzed above, when the adjustment of smart load input power  $\Delta P$  equals to  $-\Delta P_{DG}(t)$ , the fluctuation of demand side power caused by DG can be eliminated and the demand side power of ADN can be stabilized at reference value  $P_{DEM-REF}$ . Therefore, the control target of control loop can be set as

$$\Delta P = -\Delta P_{DG}(t) \quad (16)$$

Substituting (5) into (16) gives

$$\Delta P = P_{DEM} - P_{DEM-REF} \quad (17)$$

Getting the absolute value of (17) gives

$$|\Delta P| = |P_{DEM} - P_{DEM-REF}| \quad (18)$$

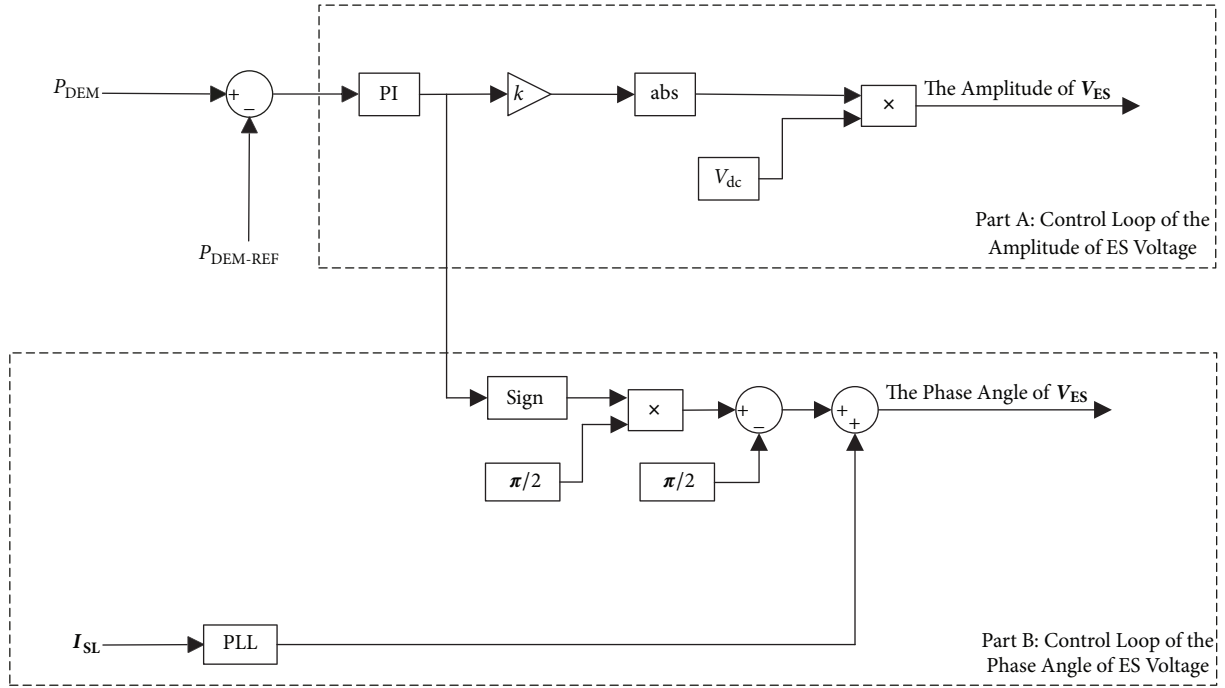


FIGURE 8: The control loop of ES voltage.

As a result, the absolute value of  $\Delta P$  should have a positive correlation with the absolute value of  $P_{\text{DEM}} - P_{\text{DEM-REF}}$ .

According to (13), it can be obtained that the amplitude of  $V_{\text{ES}}$  has a positive correlation with the absolute value of  $\Delta P$ . Therefore, combined with the conclusion above, the amplitude of  $V_{\text{ES}}$  should have a positive correlation with the absolute value of  $P_{\text{DEM}} - P_{\text{DEM-REF}}$ .

Accordingly, the amplitude of  $V_{\text{ES}}$  can be decided according to the absolute value of difference between the measured  $P_{\text{DEM}}$  and the given  $P_{\text{DEM-REF}}$ .

As a kind of linear controller, PI controller can ensure dynamic performance and steady-state performance simultaneously. Therefore, PI controller is used in this paper to control the amplitude of  $V_{\text{ES}}$ . Combined with the analysis above, the control loop of the amplitude of  $V_{\text{ES}}$  can be obtained as Part A shown in Figure 8, where  $k$  is the PI postgain,  $\text{abs}$  is the absolute value function, and  $V_{\text{dc}}$  is the DC voltage of PWM inverter.

**5.2. Control Loop of the Phase Angle of ES Voltage.** According to the control target (17),  $\Delta P$  should satisfy

$$\begin{aligned} \Delta P > 0 \quad & P_{\text{DEM}} > P_{\text{DEM-REF}} \\ \Delta P < 0 \quad & P_{\text{DEM}} < P_{\text{DEM-REF}} \end{aligned} \quad (19)$$

According to the  $0^\circ/180^\circ$  phase control strategy analyzed above, when the phase angle difference between  $V_{\text{ES}}$  and  $I_{\text{SL}}$  is  $0^\circ$ , ES works in resistive mode,  $\Delta P > 0$ , and when the phase angle difference between  $V_{\text{ES}}$  and  $I_{\text{SL}}$  is  $180^\circ$ , ES works in

negative resistive mode,  $\Delta P < 0$ . Therefore, based on (19), the phase angle difference between  $V_{\text{ES}}$  and  $I_{\text{SL}}$  should satisfy

$$\begin{aligned} \arg(V_{\text{ES}}) &= \arg(I_{\text{SL}}) + 0^\circ \quad P_{\text{DEM}} > P_{\text{DEM-REF}} \\ \arg(V_{\text{ES}}) &= \arg(I_{\text{SL}}) + 180^\circ \quad P_{\text{DEM}} < P_{\text{DEM-REF}} \end{aligned} \quad (20)$$

Based on (20), the  $0^\circ/180^\circ$  phase control loop of the phase angle of  $V_{\text{ES}}$  can be obtained as Part B shown in Figure 8, where PLL is a phase-locked loop which can output the phase of  $I_{\text{SL}}$ .

## 6. Simulation Studies

In order to verify the effectiveness of the method proposed in this paper, simulations are conducted by MATLAB/Simulink. The simulation model is shown as Figure 9, where the generation side of ADN is simulated by an AC voltage source and the random output power of DG is simulated by a PWM power inverter with prerecorded random data. There are 18 load nodes in the simulation model and the DG is set to be connected with node 15. The total loads of the 18 nodes is 15kW, in which a  $10\Omega$  load connected to node 8 is chosen as the noncritical load while other loads are critical loads. Specific parameters of the simulation model are shown in Table 1.

**6.1. ES Is Not Activated.** Switch on S in Figure 9 and conduct a 400s simulation; the demand side power waveform can be obtained as Figure 10, the output power of DG can be obtained as Figure 11, the input power waveform of noncritical load can be obtained as Figure 12(a), and the input power waveform of critical loads can be obtained as Figure 12(b). In this paper, positive value means input power, while negative value means output power.

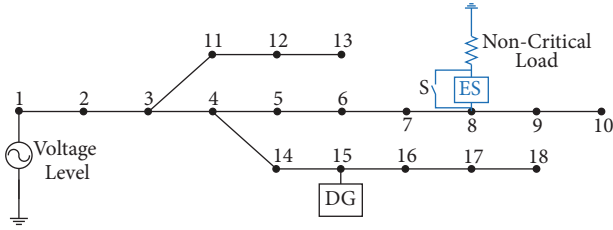


FIGURE 9: The simulation model of ADN.

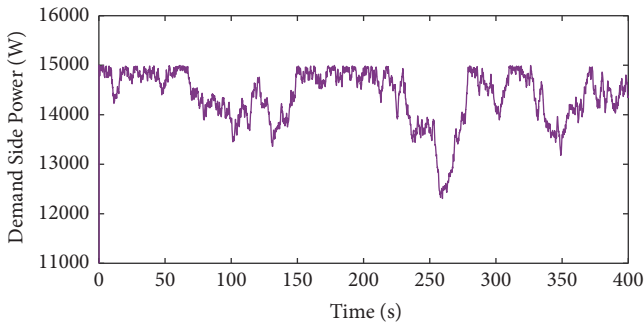


FIGURE 10: Demand side power waveform when ES is not activated.

TABLE I: Parameters of the simulation model.

Voltage level	220V
DC voltage ( $V_{dc}$ )	200V
Total loads ( $P_{Load}$ )	15kW
Non-critical load ( $R_{NC}$ )	10 $\Omega$
Inductance of the low-pass filter ( $L_f$ )	0.33mH
Capacitance of the low-pass filter ( $C_f$ )	22 $\mu$ F
Switching frequency ( $f_s$ )	20kHz
kp of PI	55
ki of PI	20
PI post-gain $k$	1/350000

As shown in Figures 10, 11, and 12, when ES is not activated, although the input power of loads is constant, the random output power of DG will cause the fluctuation of demand side power, which will bring difficulties to power dispatching.

**6.2. ES Is Activated.** As shown in Figure 11, the DG output power approximately fluctuates around 1kW. Therefore,  $P_{DG-REF}$  can be set as 1kW according to (3), and the reference value of the demand side power  $P_{DEM-REF}$  can be set as 14kW according to (4). Switch off S in Figure 9 and conduct a 400s simulation in the same environment as before; the demand side power waveform can be obtained as Figure 13, the output power of DG can be obtained as Figure 14, the smart load current waveform can be obtained as Figure 15(a), the input power waveform of smart load can be obtained as Figure 15(b), the input power waveform of noncritical load can be obtained as Figure 16(a), the input power waveform of critical loads can be obtained as Figure 16(b), the amplitude of ES voltage can be obtained as Figure 17(a), and the phase

difference between ES voltage and smart load current can be obtained as Figure 17(b).

As shown in Figures 13–17, ES can change the smart load current and the input power of loads dynamically by generating dynamical ES voltage. In this way, the fluctuation of demand side power caused by DG which is shown in Figure 10 can be balanced out and the demand side power can be stabilized approximately at the reference value 14kW as shown in Figure 13. Therefore, the difficulties of power dispatching caused by the output power fluctuation of DG can be relieved.

Moreover, as shown in Figures 14 and 15(b), the power consumption increases when the quantity of DG output power is large, while the power consumption decreases when the quantity of DG output power is small. That is, the new control paradigm where demand follows generation has been achieved by applying ES to restrain the fluctuation of demand side power in ADN.

**6.3. ES in Series with Noncritical Loads of Different Impedance Modulus.** The simulations above have verified the effectiveness of the method applying 0°/180° phase controlled ES to restrain the fluctuation of demand side power in ADN, taking ES in series with a 10 $\Omega$  noncritical load as an example. However, the selection basis of noncritical loads has been obtained in this paper, which concludes that “non-critical loads which have smaller impedance modulus should be considered to be in series with ES.” In order to verify this selection basis and provide a reference for the selection of noncritical loads in practical application, further simulations based on Figure 9 should be conducted.

Firstly, same as the above simulations, the noncritical load is set as 10 $\Omega$ . Conduct an 800s simulation; during 0–400s, ES is not activated, while during 400–800s, ES is activated on the condition that the fluctuation produced by the output power of DG is same as 0–400s. The demand side power waveform can be obtained as Figure 18(a) and the amplitude of ES voltage can be obtained as Figure 18(b). The reference value  $P_{DEM-REF}$  in this simulation is set as 14kW, which is the same as previous simulations.

Then, rechoose a noncritical load which is 9 $\Omega$ ; the demand side power waveform can be obtained as Figure 19(a) and the amplitude of ES voltage can be obtained as Figure 19(b).

Similarly, rechoose a noncritical load which is 11 $\Omega$ ; the demand side power waveform can be obtained as Figure 20(a) and the amplitude of ES voltage can be obtained as Figure 20(b).

As shown in Figures 18–20, the fluctuation of demand side power caused by DG can be restrained effectively no matter which noncritical load is in series of ES. However, the impedance modulus of noncritical load is bigger and the voltage required to be generated by ES is bigger. According to the basic principles of PWM inverter, the value range of ES voltage is constrained by the magnitude of DC voltage. Therefore, as the DC voltage is constant, in order to achieve stronger ability to restrain the fluctuation of demand side power caused by DG, noncritical loads which have smaller impedance modulus should be considered to be in series with ES firstly.

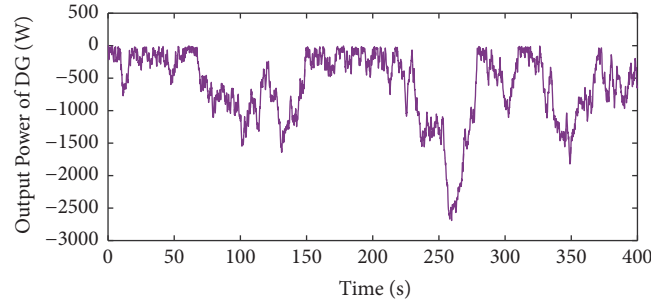


FIGURE 11: The output power waveform of DG.

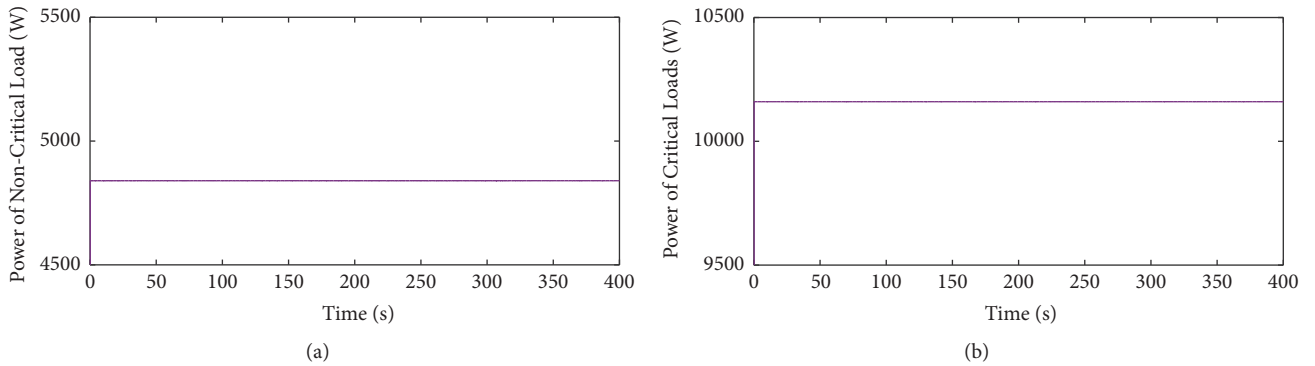


FIGURE 12: The input power waveform of loads when ES is not activated. (a) Noncritical load. (b) Critical loads.

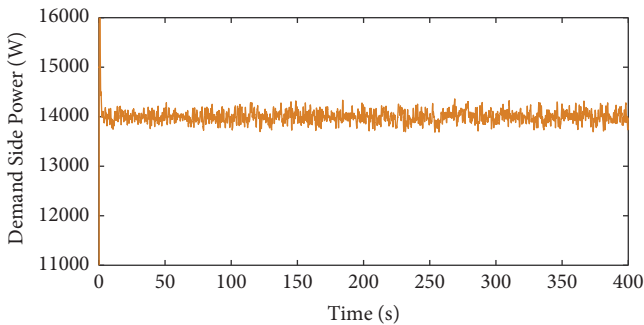


FIGURE 13: Demand side power waveform when ES is activated.

**6.4. Simulation with the Consideration of Loads Change.** As shown in the simulations above, the demand side power fluctuation caused by DG can be restrained effectively when ES is applied. However, the loads power in the above simulations is constant (15kW), which does not correspond with the actual condition in active distribution network. Therefore, the fourth simulation is conducted with the consideration of loads change, which will show the practicability of the proposed method when it is combined with the load forecasting technology in the future. The simulation model is also same as Figure 9, and the parameters are same as Table 1 except the total loads power, which is set as the solid line as shown in Figure 21.  $P_{DG-REF}$  is set as 1kW which is same as former simulations and, therefore according to (4), the

curve of  $P_{DEM-REF}$  can be obtained as the dashed line shown in Figure 21.

Firstly, ES is not activated and the demand side power waveform can be obtained as shown in Figure 22(a). Secondly, ES is activated and the demand side power waveform can be obtained as shown in Figure 22(b).

As shown in Figure 22, if ES is not activated, there is a great discrepancy between the shape of demand side power waveform and the shape of load curve as the existence of the DG output power fluctuation will bring difficulties to power dispatching. However, when ES is activated, the demand side power waveform will have quite a similar shape with the load curve and the influence of the fluctuation of DG output power can be relieved. Therefore, with the application of ES, the power dispatch can be conducted easily according to the load curve only.

## 7. Conclusion

In this paper, a method of restraining the fluctuation of demand side power in ADN is proposed, in which a new power electronic device-ES is applied by the proposed  $0^\circ/180^\circ$  phase control strategy. The control strategy has been proposed concretely, the control loop has been designed in detail, and the selection basis of noncritical loads is also obtained. Simulation results have indicated that adopting the method proposed in this paper can restrain the demand side power fluctuation caused by DG effectively, and therefore the difficulties of power dispatching caused by the output power fluctuation of DG can be relieved.

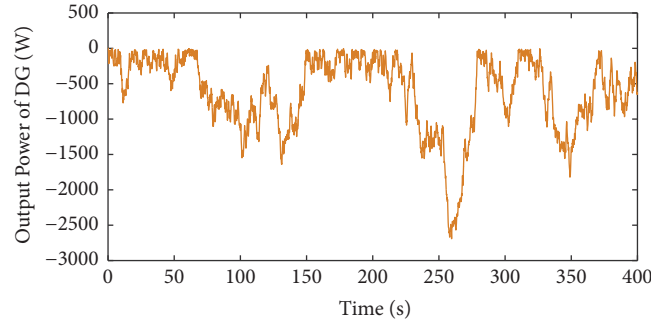
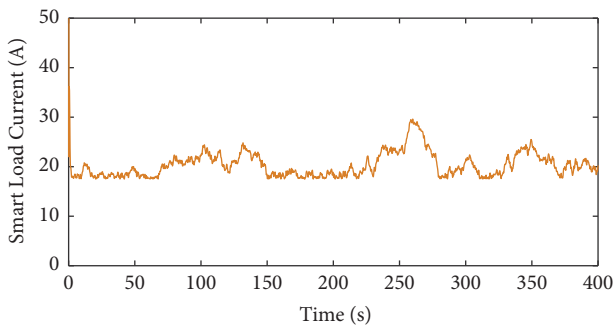
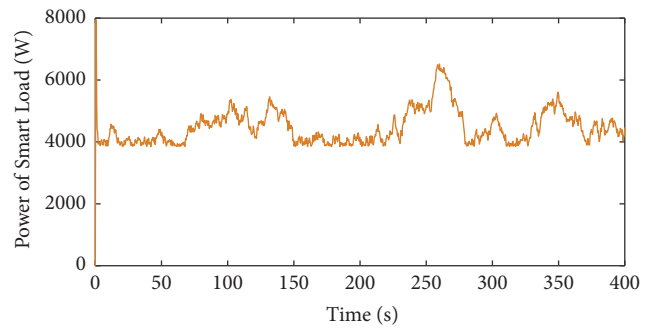


FIGURE 14: The output power waveform of DG.

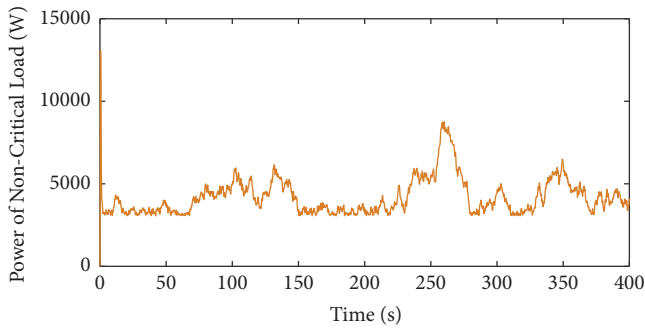


(a)

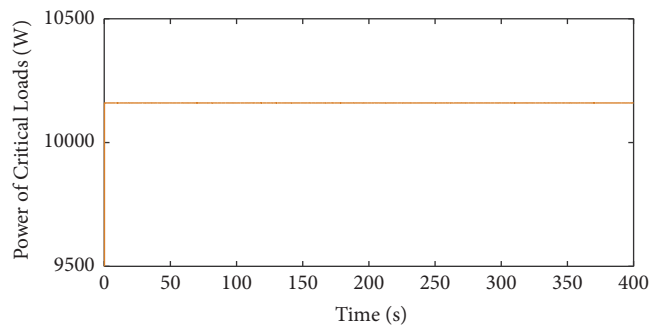


(b)

FIGURE 15: The current and input power waveform of smart load. (a) Smart load current. (b) The input power of smart load.

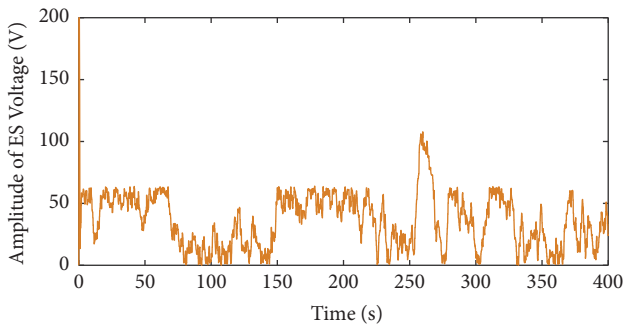


(a)

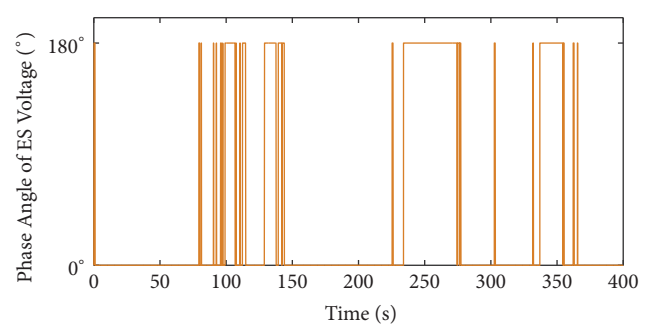


(b)

FIGURE 16: The input power waveform of loads when ES is activated. (a) Noncritical load. (b) Critical loads.



(a)



(b)

FIGURE 17: The amplitude and phase angle condition of ES voltage. (a) The amplitude of ES voltage. (b) The phase angle difference ( $0^\circ$  or  $180^\circ$ ).

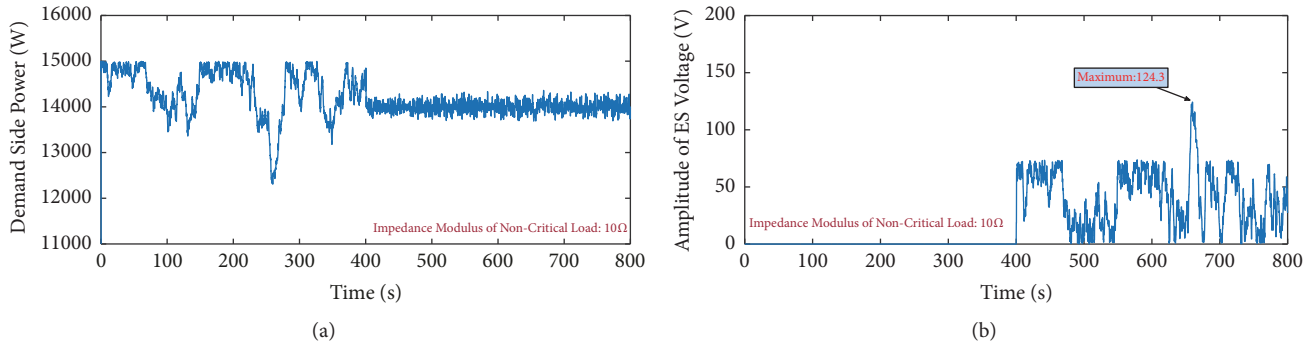


FIGURE 18: ES in series with a 10Ω noncritical load. (a) Demand side power. (b) The amplitude of ES voltage.

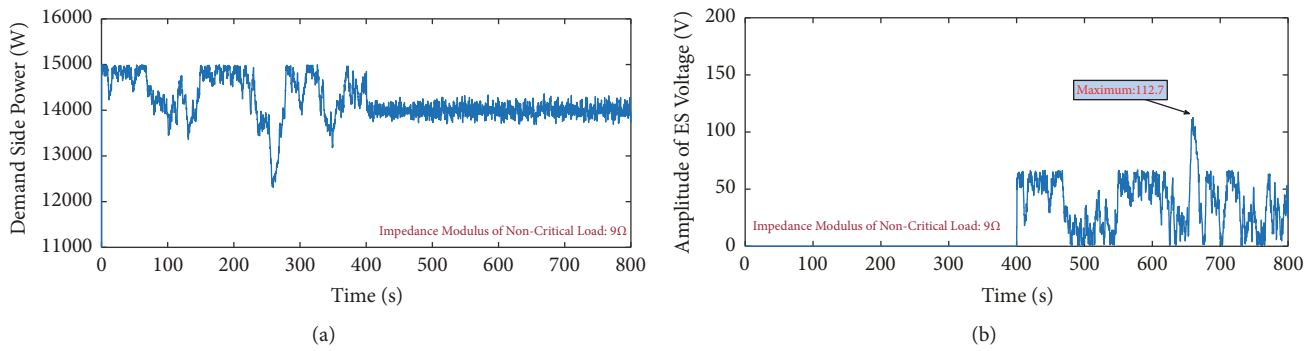


FIGURE 19: ES in series with a 9Ω noncritical load. (a) Demand side power. (b) The amplitude of ES voltage.

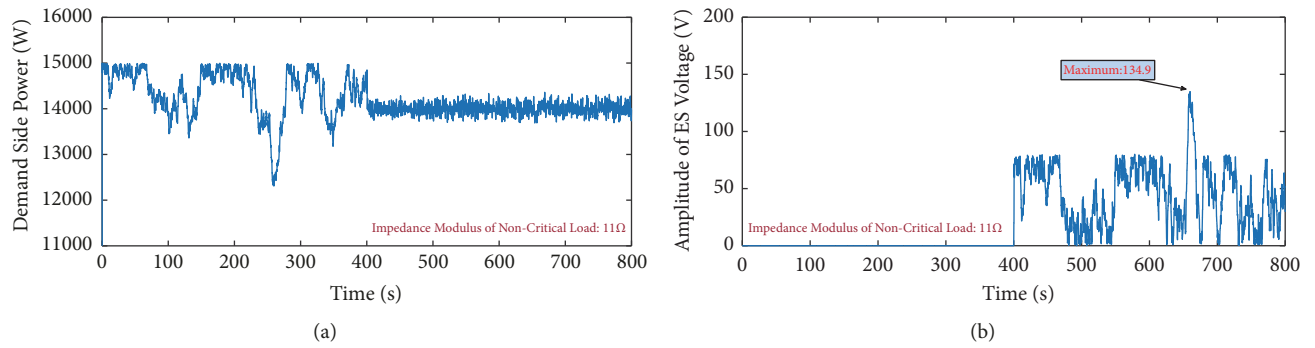


FIGURE 20: ES in series with a 11Ω noncritical load. (a) Demand side power. (b) The amplitude of ES voltage.

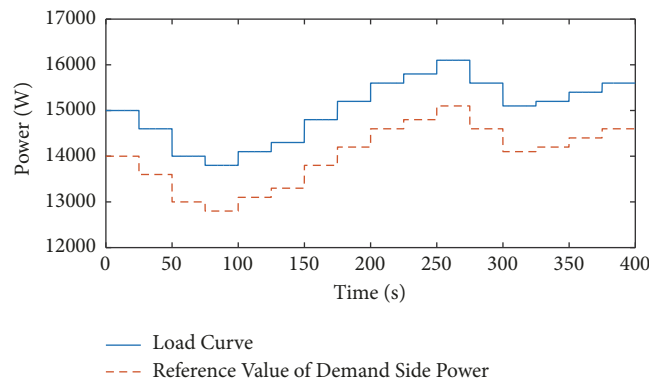


FIGURE 21: The total load curve and the reference value curve of demand side power.

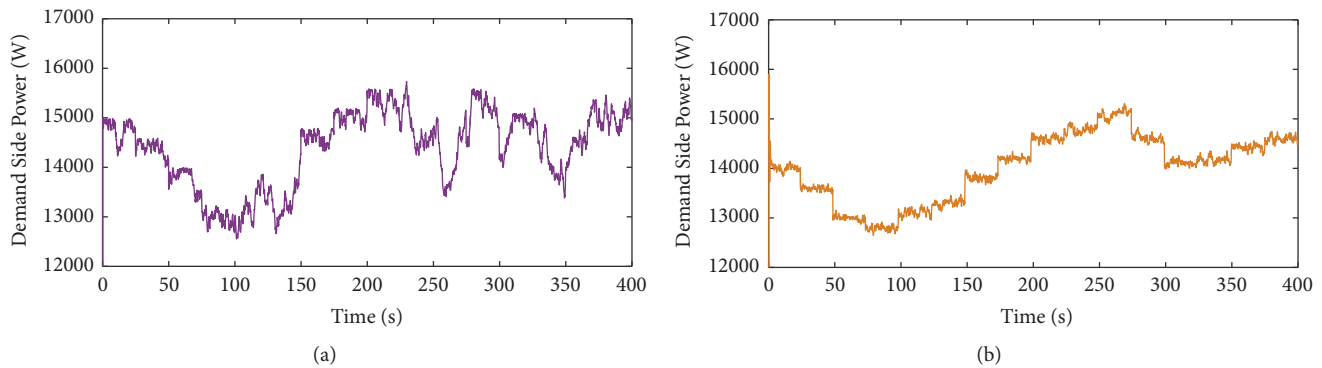


FIGURE 22: Demand side power waveform with loads change. (a) ES is not activated. (b) ES is activated.

The method proposed in this paper does not need complex communication technologies and requires easier operation. When the fluctuation of DG is big, the noncritical loads connected with ES can be added, which is more economical than the traditional way of increasing the energy storage capacity only. Besides, the new control paradigm where demand follows generation can be achieved by adopting this method. However, only one smart load is set in this paper; therefore the fluctuation of noncritical load power is not small as shown in the simulation result. To consummate the method proposed in this paper, multi smart loads should be applied to share the power fluctuation in the future, and the coordinated control strategy between them should be studied deeply.

In addition, this paper mainly uses ES to stabilize the demand side active power fluctuation in ADN. Therefore, in order to maximize the active power adjustment range, ES is not involved in the reactive power regulation. In the future, based on power decoupling technology, ES active power regulation and STATCOM reactive power regulation can be conducted simultaneously, in order to make the demand side power more flexible to be controlled.

### Data Availability

The data used to support the findings of this study are available from the corresponding author upon request.

### Conflicts of Interest

There are no conflicts of interest regarding the publication of this paper.

### Acknowledgments

This research was supported by the National Natural Science Foundation of China (51607093).

### References

- [1] G. Ma, G. Xu, Y. Chen, and R. Ju, "Multi-objective optimal configuration method for a standalone wind-solar-battery hybrid power system," *IET Renewable Power Generation*, vol. 11, no. 1, pp. 194–202, 2017.
- [2] T. Vigneysh and N. Kumarappan, "Grid interconnection of renewable energy sources using multifunctional grid-interactive converters: A fuzzy logic based approach," *Electric Power Systems Research*, vol. 151, pp. 359–368, 2017.
- [3] A. Soroudi, M. Ehsan, R. Caire, and N. Hadjsaid, "Possibilistic evaluation of distributed generations impacts on distribution networks," *IEEE Transactions on Power Systems*, vol. 26, no. 4, pp. 2293–2301, 2011.
- [4] S. Lumbreras, A. Ramos, and F. Banez-Chicharro, "Optimal transmission network expansion planning in real-sized power systems with high renewable penetration," *Electric Power Systems Research*, vol. 149, pp. 76–88, 2017.
- [5] S. S. Reddy and P. R. Bijwe, "Real time economic dispatch considering renewable energy resources," *Journal of Renewable Energy*, vol. 83, pp. 1215–1226, 2015.
- [6] C. K. Lee, B. Chaudhuri, and S. Y. Hui, "Hardware and control implementation of electric springs for stabilizing future smart grid with intermittent renewable energy sources," *IEEE Journal of Emerging and Selected Topics in Power Electronics*, vol. 1, no. 1, pp. 18–27, 2013.
- [7] G. C. Heffner, C. A. Goldman, and M. M. Moezzi, "Innovative approaches to verifying demand response of water heater load control," *IEEE Transactions on Power Delivery*, vol. 21, no. 1, pp. 388–397, 2006.
- [8] A. Brooks, E. Lu, D. Reicher, C. Spirakis, and B. Wehl, "Demand dispatch," *IEEE Power & Energy Magazine*, vol. 8, no. 3, pp. 20–29, 2010.
- [9] E. Salies, "Real-time pricing when some consumers resist in saving electricity," *Energy Policy*, vol. 59, pp. 843–849, 2013.
- [10] H. Allcott, "Rethinking real-time electricity pricing," *Resource and Energy Economics*, vol. 33, no. 4, pp. 820–842, 2011.
- [11] R. Zamora and A. K. Srivastava, "Controls for microgrids with storage: Review, challenges, and research needs," *Renewable & Sustainable Energy Reviews*, vol. 14, no. 7, pp. 2009–2018, 2010.
- [12] M. Aneke and M. Wang, "Energy storage technologies and real life applications – A state of the art review," *Applied Energy*, vol. 179, pp. 350–377, 2016.
- [13] X. Chen, Y. Hou, S.-C. Tan, C.-K. Lee, and S. Y. R. Hui, "Mitigating voltage and frequency fluctuation in microgrids using electric springs," *IEEE Transactions on Smart Grid*, vol. 6, no. 2, pp. 508–515, 2015.
- [14] C. K. Lee and S. Y. R. Hui, "Reduction of energy storage requirements in future smart grid using electric springs," *IEEE Transactions on Smart Grid*, vol. 4, no. 3, pp. 1282–1288, 2013.

- [15] Q. Wang, M. Cheng, Z. Chen, and Z. Wang, "Steady-State Analysis of Electric Springs with a Novel  $\delta$  Control," *IEEE Transactions on Power Electronics*, vol. 30, no. 12, pp. 7159–7169, 2015.
- [16] S. Yan, C.-K. Lee, T. Yang et al., "Extending the operating range of electric spring using back-to-back converter: Hardware implementation and control," *IEEE Transactions on Power Electronics*, vol. 32, no. 7, pp. 5171–5179, 2017.
- [17] S. Yan, M. Wang, T. Yang, S. Tan, B. Chaudhuri, and S. Y. Hui, "Achieving Multiple Functions of Three-Phase Electric Springs in Unbalanced Three-Phase Power Systems Using the Instantaneous Power Theory," *IEEE Transactions on Power Electronics*, vol. 33, no. 7, pp. 5784–5795, 2018.
- [18] S. Yan, M. Wang, J. Chen, and S. Y. Hui, "Smart Loads for Improving the Fault-Ride-Through Capability of Fixed-Speed Wind Generators in Microgrids," *IEEE Transactions on Smart Grid*.
- [19] S. Y. Hui, C. K. Lee, and F. F. Wu, "Electric springs - A new smart grid technology," *IEEE Transactions on Smart Grid*, vol. 3, no. 3, pp. 1552–1561, 2012.
- [20] X. Luo, Z. Akhtar, C. K. Lee, B. Chaudhuri, S.-C. Tan, and S. Y. R. Hui, "Distributed voltage control with electric springs: Comparison with STATCOM," *IEEE Transactions on Smart Grid*, vol. 6, no. 1, pp. 209–219, 2015.
- [21] S. Yan, S.-C. Tan, C.-K. Lee, B. Chaudhuri, and S. Y. R. Hui, "Use of Smart Loads for Power Quality Improvement," *IEEE Journal of Emerging and Selected Topics in Power Electronics*, vol. 5, no. 1, pp. 504–512, 2017.
- [22] N. R. Chaudhuri, C. K. Lee, B. Chaudhuri, and S. Y. R. Hui, "Dynamic modeling of electric springs," *IEEE Transactions on Smart Grid*, vol. 5, no. 5, pp. 2450–2458, 2014.
- [23] G. Ma, G. Xu, Y. Chen, and R. Ju, "Voltage stability control method of electric springs based on adaptive PI controller," *International Journal of Electrical Power & Energy Systems*, vol. 95, pp. 202–212, 2018.
- [24] T. Yang, K. T. Mok, S. Tan, C. Lee, and S. R. Hui, "Electric springs with coordinated battery management for reducing voltage and frequency fluctuations in microgrids," *IEEE Transactions on Smart Grid*, vol. 9, no. 3, pp. 1943–1952, 2018.
- [25] Z. Akhtar, B. Chaudhuri, and S. Y. R. Hui, "Smart Loads for Voltage Control in Distribution Networks," *IEEE Transactions on Smart Grid*, vol. 8, no. 2, pp. 937–946, 2017.
- [26] C. K. Lee, K. L. Cheng, and W. M. Ng, "Load characterisation of electric spring," in *Proceedings of the 5th Annual IEEE Energy Conversion Congress and Exhibition, ECCE 2013*, pp. 4665–4670, usa, September 2013.
- [27] Q. Wang, M. Cheng, Y. Jiang, W. Zuo, and G. Buja, "A Simple Active and Reactive Power Control for Applications of Single-Phase Electric Springs," *IEEE Transactions on Industrial Electronics*, vol. 65, no. 8, pp. 6291–6300, 2018.
- [28] Y. Zheng, D. J. Hill, K. Meng, and S. Y. Hui, "Critical Bus Voltage Support in Distribution Systems with Electric Springs and Responsibility Sharing," *IEEE Transactions on Power Systems*, vol. 32, no. 5, pp. 3584–3593, 2017.
- [29] S.-C. Tan, C. K. Lee, and S. Y. Hui, "General steady-state analysis and control principle of electric springs with active and reactive power compensations," *IEEE Transactions on Power Electronics*, vol. 28, no. 8, pp. 3958–3969, 2013.



**Hindawi**

Submit your manuscripts at  
[www.hindawi.com](http://www.hindawi.com)

